

Solvent Effects on AOT Reverse Micelles in Liquid and Compressed Alkanes Investigated by Neutron Spin–Echo Spectroscopy

Christopher L. Kitchens,^{*,†} Dobrin P. Bossev,[‡] and Christopher B. Roberts^{*,†}

Department of Chemical Engineering, Auburn University, Auburn, Alabama 36849, and Department of Physics, Indiana University, Bloomington, Indiana 47405

Received: June 20, 2006; In Final Form: August 17, 2006

Neutron Spin–Echo (NSE) spectroscopy has been employed to study the interfacial properties of reverse micelles formed with the common surfactant sodium bis-2-ethylhexyl-sulfosuccinate (AOT) in liquid alkane solvents and compressed propane. NSE spectroscopy provides a means to measure small energy transfers for incident neutrons that correspond to thermal fluctuations on the nanosecond time scale and has been applied to the study of colloidal systems. NSE offers the unique ability to perform dynamic measurements of thermally induced shape fluctuation in the AOT surfactant monolayer. This study investigates the effects of the bulk solvent properties, water content, and the addition of octanol cosurfactant on the bending elasticity of AOT reverse micelles and the reverse micelle dynamics. By altering these solvent properties, specific trends in the bending elasticity constant, k , are observed where increasing k corresponds to an increase in micelle rigidity and a decrease in intermicellar exchange rate, k_{ex} . The observed corresponding trends in k and k_{ex} are significant in relating the dynamics of microemulsions and their application as a reaction media. Compressed propane was also examined for the first time with a high-pressure, compressible bulk solvent where variations in temperature and pressure are used to tune the properties of the bulk phase. A decrease in the bending elasticity is observed for the d-propane/AOT/W = 8 reverse micelle system by simultaneously increasing the temperature and pressure, maintaining constant density. With isopycnic conditions, a constant translational diffusion of the reverse micelles through the bulk phase is observed, conforming to the Stokes–Einstein relationship.

Introduction

The anionic surfactant sodium bis-2-ethylhexyl-sulfosuccinate (AOT) is widely known to form stable microemulsions consisting of water, AOT, and a bulk organic solvent. In the oil rich region of the ternary phase diagram, AOT surfactant self-assembles into spherical reverse micelles with a water core on the order of a few nanometers in diameter.^{1,2} The thermodynamically stable, AOT reverse micelles are dynamic in nature consisting of translational diffusion, shape deformations, and intermicellar exchange of the aqueous cores.³ AOT reverse micelles dispersed within compressed and supercritical alkanes have been studied by a wide variety of techniques including the following: phase behavior and conductivity measurements to determine water uptake, phase transitions, and stability;^{4–7} dynamic light scattering (DLS), small-angle X-ray scattering (SAXS), and small angle neutron scattering (SANS) to determine structure and size;^{8–10} and fluorescence and solvatochromic spectroscopic methods to characterize local environments.^{11–14} In this study, the method of Neutron Spin–Echo spectroscopy (NSE) is used to determine the effects of water content and bulk solvent properties on AOT reverse micelle dynamics in hexane, cyclohexane, and compressed propane solvents with variations in temperature and pressure.

Neutron spectroscopy provides unique instrumentation for the study of colloidal systems based on the premise that neutrons are not electrically charged and interact solely with the atomic

nuclei. Neutron scattering also varies significantly between atomic isotopes whereas their chemical properties remain largely the same. This enables the use of contrast variation methods with AOT reverse micelle microemulsions consisting of deuterated water, deuterated bulk solvent, and hydrogenated AOT surfactant, such that the motions of the AOT surfactant monolayer can be selectively probed. Neutron Spin–Echo (NSE) spectroscopy is complementary to SANS, providing dynamic measurements of the scattering system while SANS relates a static representation. SANS has been widely used in studying microemulsion systems to determine the size and shape of surfactant aggregates by measuring elastic neutron scattering. NSE is a quasielastic method that measures energy transfers, in the 0.01 to 200 ns time scale, as a function of the scattering vector, Q , which depends on the space correlation of the scattering system.¹⁵ This study implements NSE to measure micellar diffusion and shape fluctuations in surfactant monolayers to studying AOT reverse micelle dynamics.^{15–21} The measured bending elasticities demonstrate the same trends observed in intermicellar exchange kinetics and nanoparticle synthesis, thus supporting the connection between the micelle interfacial properties and the application as a reaction media. Additionally, this is the first NSE investigation of reverse micelle dynamics in a high pressure, compressible bulk solvent and demonstrates the ability to control the micelle dynamics by tuning the adjustable solvent properties of the bulk solvent by using temperature and pressure.

Reverse Micelle Microemulsions

Properties of surfactant films include interfacial tension, rigidity, spontaneous curvature, saddle-splay elasticity, and

* Address correspondence to these authors. E-mail: ckitch@clemons.edu, roberts@eng.auburn.edu. Phone: (334)844-2036. Fax: (334)844-2063.

[†] Auburn University.

[‡] Indiana University.

bending elasticity, each of which are dependent on the surfactant structure, additives, ionic strength, solvent properties, and temperature.^{22–24} The Helfrich stabilization model, eq 1, relates the bending energy of a spherical microemulsion droplet to the bending elasticity k , saddle-splay elasticity \bar{k} , and the spontaneous curvature R_s .²² R_1 and R_2 are the principal curvature radii and dS is a surface area element.

$$E_{\text{bend}} = \frac{k}{2} \int dS \left(\frac{1}{R_1} + \frac{1}{R_2} - \frac{2}{R_s} \right) + \bar{k} \int dS \frac{1}{R_1 R_2} \quad (1)$$

Each of these terms contributes to the stability and structure of the emulsion. Values of k can range from fractions of $k_B T$ to $100 k_B T$. Rigid structures including membranes and lipid bilayers often fall in the 10 to $100 k_B T$ range while microemulsions and vesicle structures which are much less rigid have k values on the order of $1 k_B T$ or less.^{25,26} Values below $0.1 k_B T$ typically result in emulsion instability. The ratio \bar{k}/k is also related to the emulsion structure with \bar{k}/k between -1 and 0 yielding bicontinuous phases while values between -2 and -1 give spherical microemulsions.^{26,27} Recent studies of k for microemulsion systems have reported values of k in the 0.2 to $0.8 k_B T$ range;^{25,27,28} however, cross-researcher and cross-method comparisons often lead to inconsistencies, as will be discussed in the following sections.

The surfactant monolayer properties largely control micelle dynamics and play an important role in micelle kinetics with applications to reactions and nanomaterial synthesis. In a previous study, we demonstrated that the bulk alkane solvent and AOT surfactant tail interaction affect the growth rate of copper nanoparticles within the AOT reverse micelles via intermicellar exchange dynamics. In particular, the growth rate in cyclohexane was shown to be considerably lower than that in other n -alkane liquid solvents.²⁹ Investigations of other reaction systems, including nanoparticle synthesis, have demonstrated similar trends for the effects of the bulk solvent properties on the intermicellar exchange rate, k_{ex} .^{30,31} In particular, Fletcher et al. performed an in-depth study of the solvent effects on the k_{ex} kinetics of AOT reverse micelles, demonstrating increases in k_{ex} with increasing chain length of n -alkane solvents and significantly lower k_{ex} in cyclohexane.³ The water content of the AOT reverse micelle system, where $W = [\text{H}_2\text{O}]/[\text{AOT}]$, is related to the reverse micelle water core radius by³² r (nm) = $0.18W$ and has also been shown to influence k_{ex} , suggesting a maximum in k_{ex} and nanoparticle growth rates in the vicinity of $W = 10$.^{3,29,31,33–39}

Many of the discussions concerning intermicellar exchange rates and nanoparticle growth rates within AOT reverse micelles suggest that the physical properties of the AOT monolayer govern micelle dynamics and particle synthesis within the media. The property most commonly referred to is the micelle rigidity; however, the physical properties of surfactant monolayers also include lateral elasticity, bending elasticities, interfacial forces, and spontaneous curvature. Helfrich's model accounts for each of these contributions to the interfacial elasticity of surfactant monolayers. Values for the parameters have been determined by a variety of macroscopic and microscopic techniques with somewhat inconsistent results. Binks et al. determined the bending elasticity constant for AOT aggregates in brine systems using macroscopic interfacial tension and ellipsometry measurements and found that the bending elasticity, k , decreased with increasing chain length from n -heptane to n -tetradecane with values ranging from 1.1 to $0.6 k_B T$, respectively.⁴⁰ Other methods, including DLS and SANS, have been used to probe the properties of the AOT surfactant monolayer allowing

determination of the micelle size, shape, and polydispersity by scattering techniques.⁴¹ The polydispersity values obtained for AOT reverse micelles and other colloidal systems have been indirectly used to determine values for the bending elasticity of surfactant layers, both independently and in conjunction with other methods. The various methods used to determine the bending elasticities for the liquid-phase AOT system have resulted in inconsistencies in the values reported throughout the literature. NSE has been demonstrated to be an effective method for determination of the bending elasticity of surfactant monolayers, including the AOT reverse micelle system.

The spontaneous curvature, saddle splay elasticity, and bending elasticity can be determined from shape fluctuations in the reverse micelles which are measured by NSE. This study examines the effect of the bulk solvent and water content on the properties of the AOT reverse micelles, specifically the bending elasticity, k . The liquid alkane solvents investigated include d -hexane, d -cyclohexane, and d -decane, which are similar in composition but vary in structure, viscosity, and solvent strength. The influence of the W value on micelle dynamics is also of interest due to the demonstrated effects on the intermicellar exchange rate. Compressible fluids have the unique advantage of the tunable solvent properties which afford the ability to adjust the microemulsion properties by using temperature and pressure. The compressed propane microemulsion is thermodynamically stable over a range of temperatures and pressures allowing for adjustments in the bulk solvent thermophysical properties. The effects of varying bulk compressed propane solvent properties on the dynamics of microemulsions through changes in temperature and pressure are investigated by using neutron scattering techniques

Neutron Scattering

SANS has been used extensively in studying microemulsions as they exist in single and multiple phases to understand the thermodynamics and interaction energetics associated with phase transitions at various positions on the oil/water/surfactant ternary phase diagram.^{42–47} SANS studies were influential in determining the structure and existence of AOT microemulsions in compressed propane and ethane.^{9,10,14,48,49} Reverse micelle microemulsions are dynamic systems and describing their structure with SANS requires the use of a polydispersity term that accounts for the range of micelle diameters observed by the "static picture" of the entire microemulsion system. Equation 2 demonstrates the relationship between polydispersity and

$$p^2 = \frac{k_B T}{4\pi} \left[6(2k + \bar{k}) - 8k \frac{R_0}{R_s} - \frac{3k_B T}{2\pi} f(\phi) \right]^{-1} \quad (2)$$

spherical reverse micelles where R_0 is the mean radius, R_s is the radius of spontaneous curvature, and $f(\phi)$ is the mixing entropy per droplet as a function of the volume fraction ϕ .^{50–52} The polydispersity equation also demonstrates the contribution of the bending elasticity k and saddle-splay elasticity \bar{k} and few studies have determined values of the elastic terms using SANS measurements.^{20,53} Comparison of the bending elasticity terms obtained from SANS with those from alternative methods reveals significant inconsistencies which have been discussed in the literature.^{21,54–57} Typical values of k are on the order of $k_B T$ or smaller; however, the values obtained by SANS in the literature are generally higher.^{53,58} These inconsistencies may be a result of the static nature of the SANS measurements.^{54,59}

NSE spectroscopy measures the dynamic fluctuations of the surfactant monolayers for which the methods have been detailed

in previous literature.^{15,59} The intermediate scattering function, $I(Q,t)/I(Q,0)$, is measured by NSE and is related to an effective diffusion coefficient, D_{eff} (eq 3). The Q -dependent effective

$$\frac{I(Q,t)}{I(Q,0)} = \exp[-D_{\text{eff}}(Q)Q^2t] \quad (3)$$

diffusion is comprised of a translational diffusion coefficient, D_{tr} , and a deformation diffusion coefficient, $D_{\text{def}}(Q)$, representative of the droplet shape deformations (eq 4). The energy associated with droplet deformations resulting from thermal fluctuations in the surfactant monolayer can be used to determine the spontaneous curvature of the AOT film, the saddle-splay modulus, polydispersity of the micelles, and in particular the bending modulus of elasticity of the AOT monolayer.^{59–61}

$$D_{\text{eff}}(Q) = D_{\text{tr}} + D_{\text{def}}(Q) \quad (4)$$

$$D_{\text{def}}(Q) = \frac{5\lambda_2 f_2(QR_0) \langle |a_2|^2 \rangle}{Q^2 [4\pi [j_0(QR_0)]^2 + 5f_2(QR_0) \langle |a_2|^2 \rangle]} \quad (5)$$

with

$$f_2(QR_0) = [4j_2(QR_0) - QR_0 j_3(QR_0)]^2$$

From the Q -dependent $D_{\text{def}}(Q)$ term, eq 5 is used to determine values for the damping frequency of the droplet deformation, λ_2 , and the mean-square displacement of the 2nd mode spherical harmonics, $\langle |a_2|^2 \rangle$, where $j_n(x)$ is the n th spherical Bessel function and R_0 is the mean droplet radius.⁵⁰ The λ_2 and $\langle |a_2|^2 \rangle$ terms are obtained by fitting $D_{\text{def}}(Q)$ with eq 5 as a function of Q . λ_2 is related to the elastic properties of the reverse micelle by eq 6, which was derived by Kawabata et al.^{28,50} and is based on the model proposed by Seki et al.⁶² η is the bulk solvent viscosity and η' is the D₂O core viscosity. By using the methods of Kawabata et al.^{28,50} k is determined by eq 7 from combining eqs 2 and 6.

$$\lambda_2 = \frac{k}{\eta R_0^3} \left[4 \frac{R_0}{R_s} - 3 \frac{\bar{k}}{k} - \frac{3k_B T}{4\pi k^2} f(\phi) \right] \frac{24\eta}{23\eta' + 32\eta} \quad (6)$$

$$k = \frac{1}{48} \left[\frac{k_B T}{\pi p^2} + \lambda_2 \eta R_0^3 \frac{23\eta' + 32\eta}{3\eta} \right] \quad (7)$$

Previous neutron spectroscopy studies on AOT and other surfactant systems have concentrated mainly on microemulsion phase transitions, as well as micelle structure, dynamics, and shape fluctuations. Huang and co-workers studied the AOT reverse micelle system in decane as a function of water content for $W = 8$ to 40,¹⁸ as well as the effects of pressure and the addition of butanol cosurfactant.⁴² The bending elasticity and diffusion constant were found to be independent of W although a majority of the W values investigated were rather large compared to those studied for many applications, including nanoparticle synthesis. The addition of butanol cosurfactant to the AOT–decane system was found to result in a decrease in the bending modulus.^{42,63} Takeda and co-workers^{16,17} used NSE and observed a decrease in k with increasing temperature and decreasing pressure for the AOT reverse micelle system in decane,^{28,64,65} both as a two-phase system⁶⁴ and with $W = 18.4$.⁵⁰ An increase in pressure was found to increase the rigidity of the AOT membrane while the membrane becomes more flexible with temperature increases. In a later study it was concluded that size fluctuations and droplet diffusion are enhanced by

increasing the temperature as well as decreasing the pressure.²⁸ These results were observed with decane, a relatively incompressible fluid as the bulk solvent, which leads to an interesting question concerning the effects of temperature and pressure on the reverse micelle shape fluctuations dispersed in a compressible fluid such as propane or CO₂⁶⁶ where the solvent properties are tunable with pressure.

The goal of this study is to investigate the role of the bulk solvent and water content on the elastic properties of the AOT reverse micelle system. The deuterated bulk solvents studied include cyclohexane, hexane, decane, and compressed propane. Each of the solvents form single phase, stable reverse micelle microemulsions at the conditions investigated and regions of phase transitions were avoided. The liquid solvents, cyclohexane and hexane, were implemented as alkane solvents with the same carbon number with differences in molecular structure, density, viscosity, and strength of interaction with the AOT surfactant tails. Decane is a straight chain solvent with density and viscosity more comparable to cyclohexane than hexane. Compressed propane was investigated where temperature and pressure impact the bulk solvent properties. The influence of water content in the cyclohexane system was investigated for W values of 5, 10, and 18. Investigation of these aspects of the AOT reverse micelle system by neutron spectroscopy will provide further insight into the system and the governing properties of micelle dynamics with applications to the kinetics of nanoparticle formation.

Experimental Section

The liquid-phase microemulsions consisted of d₁₂-cyclohexane (99.5% D from Norell Inc.) or d₁₄-hexane (99% D from Sigma-Aldrich) as the bulk organic solvent, 0.137 M AOT surfactant (Sigma-Aldrich), and the necessary amount of D₂O (Norell Inc.) for the desired water content. The addition of 1-octanol (Sigma-Aldrich) at 1.0 vol % was simply added to the stable microemulsion. The resulting microemulsions were single phase, stable, clear, and colorless solutions. The solutions investigated included W values of 5, 10, and 18 in d-cyclohexane bulk solvent, $W = 10$ with d-hexane bulk solvent, and $W = 10$ in d-cyclohexane with 1.0 vol % 1-octanol. Typically W is referred to as the molar ratio of H₂O to surfactant; however, for the contrast matching neutron scattering measurements it is necessary to use D₂O and for simplicity W will be used interchangeably for both cases. Additionally, W is determined by the amount of H₂O or D₂O added to the microemulsion; the dissolved water in the solvents and AOT surfactant was assumed to be negligible.

The AOT reverse micelle microemulsion in compressed alkanes consisted of d₈-propane (98% D from Cambridge Isotope Labs) with 0.06 M AOT. The microemulsion was formed within a custom built 316 stainless steel high-pressure vessel, specifically designed and built at Auburn University for high-pressure NSE measurements. The vessel design consists of two circular sapphire windows (12.5 mm thick, 44.45 mm diameter) sealed with Viton O-rings and three 1/8 in. HiP fittings for inlet/outlet, RTD temperature control, 10 000 psi relief valve, and a Heise digital pressure gauge. The capacity of the vessel is approximately 8 mL with a path length of 6.2 mm, which was reduced to 3.0 mm with the addition of quartz spacer windows. The accessible sample area for the neutron beam was 38.1 mm in diameter to obtain the maximum signal from the 35 mm diameter neutron beam. An aluminum heating block was also constructed for temperature control with use of a silicone oil temperature bath and RTD temperature control

TABLE 1: Results Obtained from the PCF-HS Model Fit of the SANS Data for the Liquid Phase AOT Microemulsions

	d-hexane $W = 10$	d-cyclohexane $W = 5$	d-cyclohexane $W = 10$	d-cyclohexane $W = 18$	d-cyclohexane $W = 10 +$ 1.0 vol % octanol
vol fraction	0.079	0.066	0.079	0.099	0.089
av core radius (Å)	17.9	12.4	18.1	31.7	18.0
polydispersity	0.39	0.33	0.24	0.22	0.24
shell thickness (Å)	10.0	10.3	10.5	10.0	9.7
SLD contrast (Å ⁻²)	4.09×10^{-6}	3.34×10^{-6}	5.68×10^{-6}	5.91×10^{-6}	5.48×10^{-6}

device. The vessel was pressure tested to 500 bar for 48 h without rupture.

The SANS measurements were performed at the NIST Center for Neutron Research on the NG1 8m SANS with a distance of 3.6m from the sample to the 2-D area detector. The liquid-phase microemulsions were loaded in 1.0 mm path length SANS liquid sample holders. The wavelength of incident neutrons was 10 Å with a momentum transfer (Q) range from 0.006 to 0.1 Å⁻¹. The compressed propane SANS measurements were performed by using the high-pressure vessel with a path length of 3.0 mm. The wavelength of incident neutrons was 6 Å with q from 0.01 to 0.17 Å⁻¹. Data reduction and fitting was done with SANS software utilities provided by NIST.⁶⁷

The NSE measurements were performed at the NIST Center for Neutron Research on the NG5 Neutron Spin-Echo spectrometer with 6 Å wavelength neutrons and $\Delta\lambda/\lambda = 17.5\%$. Measurements included the samples, backgrounds (vessel + solvent at each condition) and CarboPac (completely inelastic scattering sample to measure instrument resolution) at each of the Q values, and the percent transmission of the neutron beam for each sample. The detector was positioned at four different scattering angles to encompass the desired Q ranges. Fourier times were determined by the decay rate of the intermediate scattering function and collection times were determined by the intensity of the scattered neutrons.

Results and Discussion

SANS Measurements. The liquid alkane phase AOT reverse micelle microemulsion was investigated by using SANS with hexane as the bulk solvent and $W = 10$, as well as in cyclohexane with $W = 5, 10$, and 18. The addition of 1.0 vol % 1-octanol cosurfactant to cyclohexane with $W = 10$ was also investigated. The reverse micelle system studied consists of deuterated bulk solvent and water core that are contrast matched to isolate the hydrogenated surfactant shell. The reverse micelle neutron scattering intensity was modeled with a poly core form factor (polydisperse spherical particles with a core shell structure) and a hard sphere structure factor (hard sphere interparticle interactions), built into the NCNR data analysis software.⁶⁷ The variables taken into account by the poly core form-hard sphere (PCF-HS) model include the micelle volume fraction, average core radius (Å), polydispersity, shell thickness (Å), scattering length density (SLD) of the core (Å⁻²), shell SLD (Å⁻²), solvent SLD (Å⁻²), and the background (cm⁻¹). The terms held constant during the fitting of the SANS data include the micelle volume fraction determined from the experimental conditions, the shell SLD for AOT at 6.42×10^{-7} Å⁻² as obtained from the literature,⁶⁸ and the solvent SLD at values of 6.7×10^{-6} and 6.14×10^{-6} Å⁻² for d-cyclohexane and d-hexane, respectively.⁶⁹

The background values were measured by the scattering of the pure solvents over the Q range and were fixed at 0.08 cm⁻¹ for d-cyclohexane and 0.1 cm⁻¹ for d-hexane. The average core radius, polydispersity, shell thickness, and core SLD were determined from the model fitting. For the case of the d-hexane

$W = 10$ system, it was necessary to fix the shell thickness to obtain acceptable results from the model and a shell thickness of 10 Å was assumed based on the cyclohexane results and previously reported values.¹ The D₂O core SLD was allowed to vary during the curve fitting and an initial value of 6.37×10^{-6} Å⁻² was used. The results obtained from the data fitting confirm the core-shell structure and are listed in Table 1 and the reverse micelle radius is obtained from the sum of the core radius and the shell thickness. An expected decrease in core radius with decreasing W is observed, as well as a decrease in the SLD of the core which may be the result of an increased influence of the surfactant headgroup or the presence of hydrogenated water that was not removed during surfactant drying. The polydispersity is influenced by the bulk solvent as well as the water content at low W values. An increased polydispersity was observed with d-hexane as the bulk solvent, compared to d-cyclohexane. An increase in polydispersity is also observed in d-cyclohexane with $W = 5$ compared to $W = 10$ and 18. Interestingly, the addition of 1.0 vol % octanol, known to act as a cosurfactant, had negligible effect on the polydispersity and micelle size. In contrast, the addition of butanol cosurfactant to the AOT-decane reverse micelle system was reported to increase the polydispersity.⁴²

SANS for the AOT/d-propane/D₂O microemulsion was investigated with $W = 3$, [AOT] = 0.06 M, temperatures of 20 and 35 °C, and pressures of 138, 241, and 345 bar with solvent densities ranging from 11.57 to 12.63 mol/L. The SANS data reveal very little change with temperature and pressure with a slight increase in scattering intensity at the higher temperature. The data were fit with the PCF-HS model, as well as a poly core form factor (PCF) model that neglects any interparticle interactions by setting $S(Q) = 1$. Both models fit the data well with a reverse micelle radius of ~ 16 Å within ± 0.05 Å, polydispersity of 0.62 within ± 0.04 , and background values consistent with the measured values. The closeness of fit for the two models demonstrates the relative weakness of interparticle interactions, confirming the observations of Eastoe et al. for the AOT/h-propane/D₂O system with $W = 20$ and polydispersity values for the D₂O core on the order of 0.20.⁹ The SANS results obtained for the d -propane/ $W = 3$ microemulsion correspond well with the previous studies in compressed h-propane.^{9,14,48}

Liquid-Phase NSE Measurements. Liquid-phase AOT reverse micelle microemulsions corresponding to those studied by SANS were investigated by using NSE and Figure 1 displays the intermediate scattering function, $I(Q,t)/I(Q,0)$, decay curves for various Q values. A majority of the measured decay curves were eliminated for clarity of presentation. An indication of the micelle dynamics can be inferred from the decay rates where an increased decay is observed with a decrease in solvent viscosity from d-cyclohexane to d-hexane and with a decrease in micelle radius at lower W values. The increased decay rate is indicative of increased micellar effective diffusion where the $I(Q,t)/I(Q,0)$ data are fit by eq 3 resulting in the Q -dependent D_{eff} shown in Figure 2. The diffusion curves demonstrate a

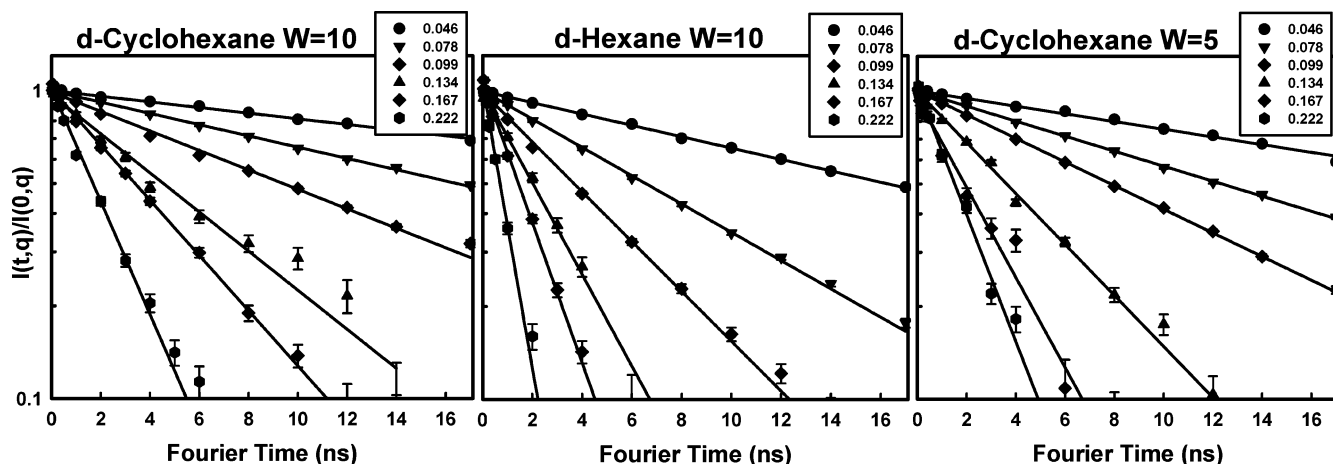


Figure 1. The intermediate scattering function decay curves measured by NSE for the liquid-phase AOT microemulsions for (a) d-cyclohexane $W = 10$, (b) d-hexane $W = 10$, and (c) d-cyclohexane $W = 5$. The solid lines are fits of the data to obtain D_{eff} for each Q .

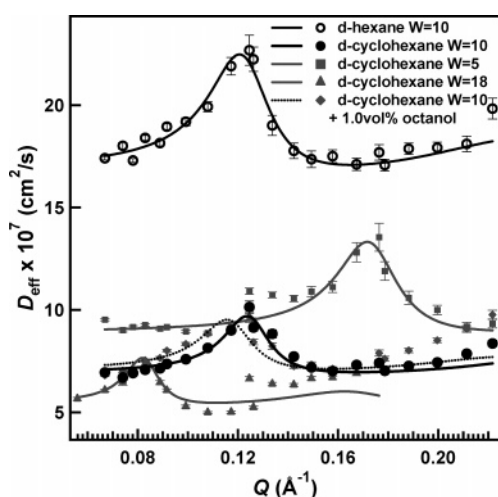


Figure 2. Q -dependent diffusion results obtained by NSE for the liquid-phase AOT reverse micelle microemulsion. The solid lines represent the fitting of the data points with eqs 4 and 5.

Q -independent translational diffusion term, D_{tr} , and a distinct Q -dependent peak that accounts for the deformation diffusion, D_{def} . The reverse micelle size and the viscosity of the bulk solvent impact the D_{tr} , which corresponds with the Stokes–Einstein relation, given in eq 8 where η is the bulk viscosity.

$$D_{\text{tr}} = \frac{(1 - \phi)k_{\text{B}}T}{6\pi\eta R_{\text{H}}} \quad (8)$$

The viscosity of the deuterated solvents was estimated from the viscosity of the hydrogenated solvent analogues with density adjustments, assuming the force independent, kinematic viscosity of the deuterated solvents is equivalent to that of the hydrogenated solvents. In the same respect, the Stokes–Einstein relation can be used to determine a correlation length, ξ_{r} , from the measured D_{tr} by eq 9. ξ_{r} has been used to determine the degree

$$\xi_{\text{r}} = \frac{(1 - \phi)k_{\text{B}}T}{6\pi\eta D_{\text{tr}}} \quad (9)$$

of interparticle interactions between the reverse micelles in solution by differences in ξ_{r} and the micelle radius.¹⁰ A correlation length, ξ_{r} , greater than the micelle radius suggests increased interparticle interactions which are influential in micelle dynamics. Table 2 lists the results obtained from the

NSE measurements as well as a comparison of the micelle radii determined by NSE, SANS, and the correlation length. The micelle radii predicted by SANS are consistently higher than NSE but show very good agreement. Comparison of ξ_{r} and the micelle radii shows excellent agreement for the reverse micelles in d-cyclohexane; however, for d-hexane, ξ_{r} suggests a slightly increased interparticle interaction. This increase may be explained by a decrease in the solvent interaction with the AOT tails as the bulk solvent is changed from d-cyclohexane to d-hexane. The solvent interaction can be characterized by the Hildebrand chi interaction parameter, χ , of 0.011 for cyclohexane–AOT and 0.11 for hexane–AOT where the AOT solubility parameter is calculated by the Hoy group contribution method.^{29,70} The greater χ for the hexane system would suggest enhanced self-association of the AOT surfactant tails due to the decreased solvent–tail interactions.

The Q -dependent D_{def} contribution to the diffusion curves contains two distinct pieces of information, the position of the peak, $Q [D_{\text{eff}}(\text{max})]$, and the relative intensity, $D_{\text{eff}}(\text{max})/D_{\text{tr}}$. The peak position is significant because it is identical with the Q -dependent relation ($\pi/\text{micelle radius}$) as demonstrated in Table 2. In a similar NSE study by Hirai et al. on AOT microemulsions in d-heptane with $W = 5, 10, \text{ and } 20$ it was concluded that at low W , the predicted $Q [D_{\text{eff}}(\text{max})] = \pi/R$ relation does not hold true.¹⁶ In contrast, this study with d-hexane and d-cyclohexane as the bulk organic solvent demonstrates convincingly that the semiempirical relation does hold true.^{18,51,53} The intensity of the D_{def} peak increases with increasing micellar dynamics, including D_{tr} . Previous studies have suggested that the relative intensity of this peak is related to the dynamic properties of the surfactant monolayer^{18,51} as discussed below.

Table 2 lists the AOT monolayer bending elasticity determined by eq 7 with the SANS polydispersity and NSE dampening frequency, λ . The dimensionless bending elasticity constants, $k/k_{\text{B}}T$, are acceptable in that they are positive and less than 1, corresponding closely with accepted values.^{54,58} Values of k in the $0.2 k_{\text{B}}T$ range are representative of surfactant films in nonrigid systems. These systems are very dynamic in nature as demonstrated by measurements of the intermicellar exchange kinetics.^{3,29,33} One example is the bending elasticity constants measured by Binks et al.⁴⁰ using ellipsometry for the AOT emulsion in various alkane solvents, observing a transition from lamellar to bicontinuous organization ($\sim 1.0 k_{\text{B}}T$ to $0.06 k_{\text{B}}T$). In contrast, the values obtained in this study are generally less than values measured by SANS methods both independently and in conjunction with DLS.^{19,21,54,59,71} Granted, the differences

TABLE 2: NSE Results for the Liquid Phase Microemulsions and Comparison of the Reverse Micelle Radius Determined by SANS, NSE, and the Correlation Length^a

	d-hexane $W = 10$	d-cyclohexane $W = 5$	d-cyclohexane $W = 10$	d-cyclohexane $W = 18$	d-cyclohexane $W = 10 +$ 1.0 vol % octanol
damping freq (Hz)	7.97×10^7	1.29×10^8	4.22×10^7	1.48×10^7	3.24×10^7
amplitude	1.32×10^{-2}	7.06×10^{-3}	7.78×10^{-3}	9.30×10^{-3}	1.06×10^{-2}
$Q[D_{\text{eff}}(\text{max})]$ (\AA^{-1})	0.120	0.170	0.124	0.082	0.116
π/R	0.122	0.173	0.125	0.083	0.117
$D_{\text{tr}} \times 10^7$ (cm^2/s)	17.1	9.0	7.0	5.5	7.1
R (\AA) (NSE)	25.7	18.2	25.2	38.0	26.9
R (\AA) (SANS)	27.9	22.8	28.6	41.7	27.7
corr length ξ (\AA)	32.2	20.1	25.6	32.0	24.8
$k/k_{\text{B}}T$	0.19	0.23	0.22	0.26	0.19

^a The values for the bending elasticity modulus demonstrate trends consistent with micelle dynamics.

in $k/k_{\text{B}}T$ for the liquid-phase systems are small; the relative trends observed correspond well with the predictions of micelle rigidity as seen by micelle dynamics studies. As the bulk solvent is changed from d-cyclohexane to d-hexane, $k/k_{\text{B}}T$ decreases from 0.22 to 0.19 and thus a decrease in the bending elasticity would correspond to a decrease in the micelle rigidity. The addition of 1.0 vol % octanol cosurfactant to the d-cyclohexane $W = 10$ microemulsion also resulted in a decrease in $k/k_{\text{B}}T$, corresponding to a decrease in micelle rigidity. The addition of 5 vol % octanol to the d-cyclohexane, $W = 10$ microemulsion resulted in decreased stability of the microemulsion and a two-phase system. These observations are consistent with a decrease in the bending modulus observed with the addition of butanol to the decane/AOT microemulsion by Farago.⁴² The effect of W on $k/k_{\text{B}}T$ is also small with a minimum observed for $W = 10$. This suggests an increase in micelle rigidity would exist at both lower and higher W values. Explanation of the observed trends in k as a function of W is most likely a result of deviation from the surfactant spontaneous curvature as well as the ionic interactions between the surfactant headgroups at low W values where the existence of bulk water is minimal. Despite the small changes in $k/k_{\text{B}}T$, the observed trends correspond with previously observed solvent and water content effects on micelle dynamics measured by the intermicellar exchange rate where a decrease in micelle bending elasticity or rigidity would result in an increased intermicellar exchange rate.^{3,33,72}

The bending elasticity constants for the AOT surfactant monolayer have been determined by other techniques. The most commonly referenced study by Binks et al. used ellipsometry to determine k for AOT in the lamellar phase and reported values of $1 k_{\text{B}}T$ with heptane, octane, and decane as the oil phase at 20 °C. As the oil phase increased in carbon number to undecane, dodecane, and tetradecane, k decreased to 0.4, 0.16, and 0.06, respectively, as a transition to a bicontinuous phase was observed.^{40,58} In another study, Nagao et al. used NSE and SANS to study the decane/AOT microemulsion in the dense droplet regime with equal volume fractions of D_2O and n -decane at 25 °C and reported $k = 1.4 k_{\text{B}}T$.⁶⁴ The d-decane/AOT reverse micelle system has also been investigated with defined W values including the initial study by Huang et al. in 1987, who reported $k \sim 5 k_{\text{B}}T$ using NSE.¹⁸ The d-decane/AOT/ D_2O microemulsion has since then been studied by using NSE by Farago et al. [$k = 3.0 k_{\text{B}}T$ with $W = 24.5$ ⁶³ and $k = 3.8 k_{\text{B}}T$ with $W = 24.4$]⁴² and by Kawabata et al. with similar methods to this study [$k = 0.3 k_{\text{B}}T$ with $W = 18.4$].^{28,50}

The d-decane/AOT/ $W = 18.4$, $T = 20$ °C, reverse micelle system was also studied on the NG5 NSE spectrometer at the NCNR during the 2003 NCNR Summer School on Methods and Applications of Neutron Spectroscopy. Results from this

study yielded the following: $\lambda_2 = 1.77 \times 10^7$, $\langle |a_2|^2 \rangle = 8.64 \times 10^{-3}$, $D_{\text{tr}} = 4.5 \text{ \AA}^2/\text{ns}$, $R(\text{NSE}) = 39.2 \text{ \AA}$, $R(\text{SANS}) = 42.0 \text{ \AA}$, polydispersity = 0.25, $\xi_{\text{r}} = 40.5$, and $k = 0.22 k_{\text{B}}T$. This k value is comparable to those obtained by Kawabata and again is low with respect to other values listed in the literature for the AOT reverse micelle system, but is very consistent with the values determined in this study and other microemulsion systems.²⁷ The k determined for d-decane/ $W = 18.4$ is less than that for d-cyclohexane/ $W = 18$, suggesting a less rigid micelle would be formed with decane as the bulk solvent, as compared to cyclohexane. The reverse micelle radii determined in the two systems by SANS and NSE show excellent agreement. A correlation length greater than the micelle radius suggests interparticle interaction which may be expected based on microemulsion stability and an accessible phase transition around 60 °C.⁵⁰ The D_{tr} values obtained for d-cyclohexane and d-decane also correspond nicely for micelles of comparable size in bulk solvents with similar viscosities.

A wide range of values for k have been determined from different researchers, instrumentation, and methods. Many of these methods are very indirect and in order to determine k , one must apply theories of varying depth and numerous assumptions which lead to differences in the results. NSE is a dynamic method that determines k through thermal fluctuations in the surfactant monolayer as opposed to structural methods that use shape polydispersity such as SANS. Continued development of instrumental methods and theory will lead to better understanding of surfactant films as they apply to applications such as reaction systems.

In all, the bending elasticity constant trends measured with respect to bulk solvent and water content are significant, particularly when correlated with the intermicellar exchange rate, k_{ex} , which has applications in controlling chemical reactions and nanoparticle synthesis within these systems. The rates of chemical reactions mediated within the cores of reverse micelles, such as metallic nanoparticle synthesis, are governed by the intermicellar exchange process, where the contents of the aqueous cores of two reverse micelles are exchanged. Investigation of chemical reaction rates by Fletcher et al.³ demonstrated a decrease in the k_{ex} with decreasing chain length of liquid n -alkane bulk solvents and significantly lower k_{ex} in cyclohexane. Similar trends in bulk solvent effects on growth rates were observed in our studies of copper nanoparticle synthesis,²⁹ as well as the synthesis of cadmium sulfide quantum particles by Towey et al.³⁴ Additional studies on k_{ex} and reverse micelle mediated reactions, including Fletcher et al. and our study on copper nanoparticle synthesis, have demonstrated a decrease in k_{ex} or particle growth rate with increasing water content with $W > 10$.^{3,29,31,33,34} Other studies have demonstrated a decrease

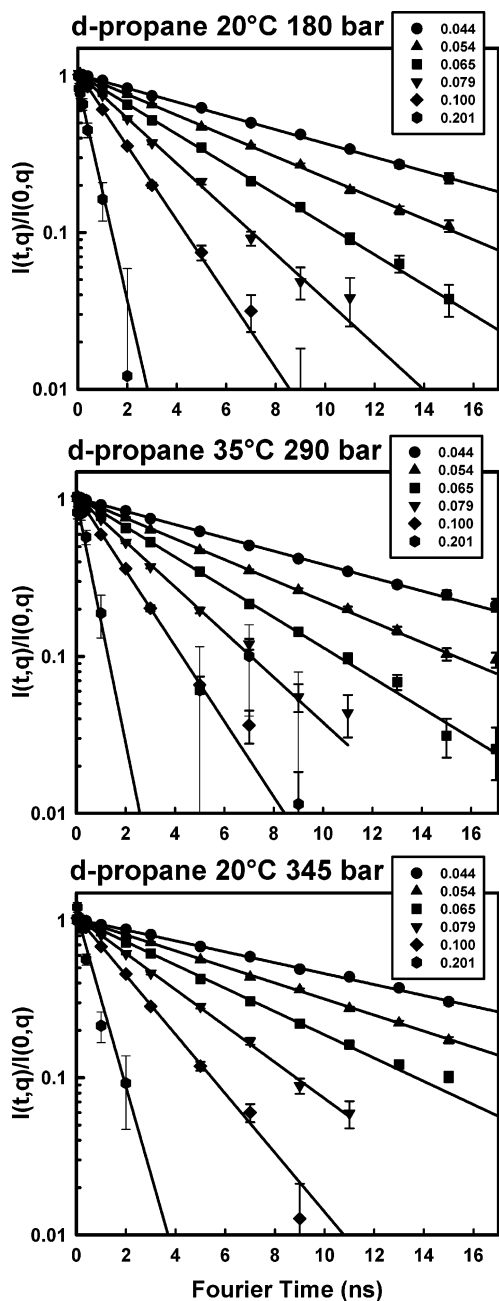


Figure 3. The intermediate scattering function decay curves measured by NSE for the compressed d-propane/AOT/ $W = 8$ microemulsions. The solid lines are fits of the data to obtain D_{eff} for each Q . Data for a limited number of Q values are presented for simplicity.

in the exchange and growth rates as the water content is decreased with $W < 10$.^{3,33–39} Comprehensive review of these results suggests a maximum in the exchange and growth rates in the vicinity of $W = 10$, which correlate nicely with this study. Given that an increase in k_{ex} results from a decrease in micelle rigidity or a decrease in the bending elasticity constant, the NSE results are in complete agreement with the results observed with reaction rate applications.

Compressed Propane Phase NSE Measurements. Figure 3 is the incoherent scattering function decay measured by the NSE spectrometer for the compressed d-propane/AOT/ $W = 8$ reverse micelle microemulsion at three conditions of varying temperature and pressure. Only a select few of the measured curves at the different Q values are shown for clarity. Figure 4 displays the Q -dependent D_{eff} results obtained from the decay fits in Figure 3. The results at 20 °C, 180 bar and 35 °C, 290

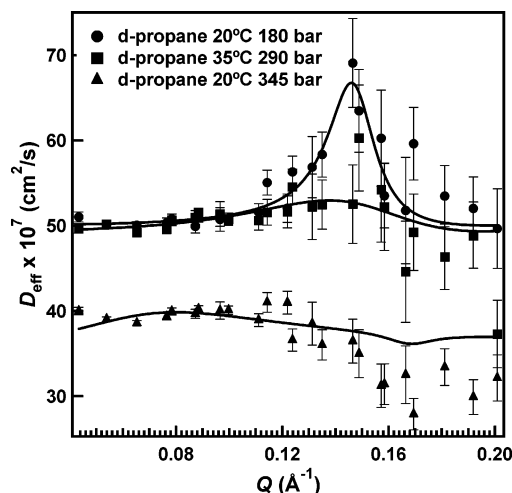


Figure 4. Q -dependent diffusion results obtained by NSE for the compressed d-propane/AOT/ $W = 8$ reverse micelle microemulsion.

TABLE 3: NSE Results for the Compressed d-Propane/AOT/ $W = 8$ Microemulsions as a Function of Temperature and Pressure

d-propane/AOT/ $W = 8$	20 °C 180 bar	35 °C 290 bar	20 °C 345 bar
damping freq (Hz)	3.59×10^8	7.26×10^7	3.60×10^7
amplitude	5.40×10^{-3}	4.53×10^{-2}	4.34×10^{-1}
$D_{\text{tr}} \times 10^7$ (cm ² /s)	50.0	49.3	36.1
R (Å)	21.4	21.7	25.1
corr length ξ (Å)	26.8	28.4	31.4
$k/k_{\text{B}}T$	0.37	0.19	0.20

bar demonstrate the effects of increased temperature and pressure such that the density and viscosity are matched with values of 0.536 g/mL and 0.156 cP, respectively. The NSE results at these conditions yielded excellent results with a distinct peak where $Q [D_{\text{eff}}(\text{max})] = \pi/R$ and nearly identical values for D_{tr} , as would be expected given the matched bulk solvent viscosity. The NSE results at 20 °C and 345 bar are questionable where the expected peak in the D_{eff} curve was not observed. The results do indicate expected behavior in the low Q range with a decrease in D_{tr} with the elevated pressure and increased density, corresponding to a higher viscosity of 0.184 cP for the bulk solvent. The NSE results presented in Table 3 for measurements at 20 °C, 180 bar and 35 °C, 290 bar demonstrate a decrease in the damping frequency, λ_2 , and an increase in $\langle |a_2|^2 \rangle$ with increased temperature and pressure. Additionally, excellent agreement was observed for the reverse micelle radius, D_{tr} , and the $Q [D_{\text{eff}}(\text{max})] \sim \pi/R$ relationship. Values of π/R and $D_{\text{eff}}(\text{max})$ for 20 °C, 180 bar were 0.147 and 0.146 and for 35 °C, 290 bar they were 0.145 and 0.140, respectively. The NSE temperature and pressure study for d-decane/AOT/ $W = 18.4$ by Kawabata et al. showed that $\langle |a_2|^2 \rangle$ increased with temperature and decreased with pressure, indicating that the micelle shape fluctuations are enhanced with increasing temperature and suppressed with increasing pressure.⁵⁰ This study demonstrates an increase in $\langle |a_2|^2 \rangle$ with increased temperature and pressure at a constant bulk solvent viscosity, suggesting a greater effect of temperature on shape fluctuations, which was also observed by Kawabata.⁵⁰ The calculated correlation length is similar to the micelle radius indicating minimal interparticle interaction as expected for a stable microemulsion at conditions far from a phase transition.^{9,10}

The values for k listed in Table 3 were determined by using eq 7 and polydispersity values of 0.25, 0.21, and 0.21 for the three conditions with increasing pressure measured by SANS on the d-propane/AOT/ $W = 3$ microemulsion. Assuming the

polydispersity for $W = 3$ and 8 is the same in the d-propane system, a decrease in k is observed with increasing T and P at constant density. Determination of the bending elasticity constant assuming a constant polydispersity of 0.20^9 yields values of $0.43 k_B T$ at 20°C , 180 bar and $0.20 k_B T$ at 35°C , 290 bar. In the case that a polydispersity of 0.30 is used, slightly lower values of $0.34 k_B T$ and $0.11 k_B T$ are obtained which exhibit the same decreasing trend. Previous NSE studies of temperature and pressure effects on the AOT microemulsion system include the Kawabata study and the previously mentioned Nagao study of n -decane in the dense droplet regime. Nagao et al. found that k decreased from $1.4 k_B T$ to $0.4 k_B T$ with an increase in temperature from 25 to 40°C at 1 bar and increased to $2.6 k_B T$ with an increase in pressure from 1 to 600 bar at 25°C .⁶⁴ Kawabata et al. also reported a decrease in k with increasing temperature and an increase in k with increasing pressure.⁵⁰ For both studies of the relatively incompressible n -decane system, the influence of pressure on k was greater than that of temperature. For the d-propane system, a decrease in k with simultaneous increases in temperature and pressure suggests that temperature may influence k more so than pressure despite the compressible nature of the bulk fluid. Moreover, this study demonstrates the ability to measure reverse micelle dynamics in a compressed d-propane microemulsion system and the ability to adjust the surfactant interfacial properties with the tunable properties of the bulk compressible fluid by using temperature and pressure.

Conclusions

This work demonstrates the effects of the bulk solvent, water content, and octanol cosurfactant on the AOT reverse micelle system by measuring shape fluctuations to determine the bending elasticity of the surfactant monolayer. The results revealed subtle differences in the bending elasticity for each of the liquid systems investigated; however, the trends observed correspond very well with the results obtained by alternative methods of studying AOT reverse micelle dynamics, particularly microemulsion stability, intermicellar exchange rates, and nanoparticle growth kinetics. The bending elasticity constants are relatively low compared to the diverse range of values listed in the literature, but are consistent with theoretical approximations. Moreover, the observed increasing trends in bending elasticity correspond to increases in micelle rigidity and decreasing intermicellar exchange in the liquid-phase AOT microemulsion, depending on the bulk solvent, water content, and cosurfactant presence.

To our knowledge, this is the first NSE study of temperature and pressure effects on a microemulsion formed within a compressible solvent. The measurements performed on the compressed propane/AOT/ $W = 8$ reverse micelle system demonstrate the use of a tunable solvent to adjust the properties of the reverse micelle surfactant monolayer without changing the density or viscosity of the bulk fluid. This affords the ability to alter the micelle rigidity while maintaining constant translational diffusion through the bulk fluid, or vice versa. The ability to control the surfactant interfacial properties by adjusting the bulk fluid properties with temperature and pressure in a compressible fluid offers significant opportunity when applied as a synthesis media.

Acknowledgment. The authors would like to thank the NCNR instrument scientists and staff who provide an excellent work environment for visiting researchers. We gratefully acknowledge the financial support provided by the Department

of Energy-Basic Energy Sciences (DE-FG02-01ER15255). This work utilized facilities supported in part by the National Science Foundation under Agreement No. DMR-0086210. We acknowledge the support of the National Institute of Standards and Technology, U.S. Department of Commerce, in providing the neutron research facilities used in this work.

References and Notes

- (1) Nave, S.; Eastoe, J.; Heenan, R. K.; Steyler, D.; Grillo, I. *Langmuir* **2000**, *16*, 8741.
- (2) Mittal, K. L.; Kumar, P. *Handbook of microemulsion science and technology*; Marcel Dekker: New York, 1999.
- (3) Fletcher, P. D. I.; Howe, A. M.; Robinson, B. H. *J. Chem. Soc., Faraday Trans. 1* **1987**, *83*, 985.
- (4) Fulton, J. L.; Smith, R. D. *J. Phys. Chem.* **1988**, *92*, 2903.
- (5) Smith, R. D.; Fulton, J. L.; Blitz, J. P.; Tingey, J. M. *J. Phys. Chem.* **1990**, *94*, 781.
- (6) McFann, G. J.; Johnston, K. P. *J. Phys. Chem.* **1991**, *95*, 4889.
- (7) Martin, T. M.; Solvason, C. C.; Roberts, C. B. *J. Chem. Eng. Data* **2001**, *46*, 769.
- (8) Blitz, J. P.; Fulton, J. L.; Smith, R. D. *J. Phys. Chem.* **1988**, *92*, 2707.
- (9) Eastoe, J.; Steyler, D. C.; Robinson, B. H.; Heenan, R. K. *J. Chem. Soc., Faraday Trans.* **1994**, *90*, 3121.
- (10) Eastoe, J.; Young, W. K.; Robinson, B. H.; Steyler, D. C. *J. Chem. Soc., Faraday Trans.* **1990**, *86*, 2883.
- (11) Gale, R. W.; Fulton, J. L.; Smith, R. D. *J. Am. Chem. Soc.* **1987**, *109*, 920.
- (12) Roberts, C. B.; Thompson, J. B. *J. Phys. Chem. B* **1998**, *102*, 9074.
- (13) Johnston, K. P.; McFann, G. J.; Peck, D. G.; Lemert, R. M. *Fluid Phase Equilib.* **1989**, *52*, 337.
- (14) Eastoe, J.; Robinson, B. H.; Visser, A.; Steyler, D. C. *J. Chem. Soc., Faraday Trans.* **1991**, *87*, 1899.
- (15) Rosov, N.; Rathgeber, S.; Monkenbusch, M. Neutron Spin-Echo spectroscopy at the NIST Center for Neutron Research. In *Scattering From Polymers*; American Chemical Soc: Washington, DC, 2000; Vol. 739, p 103.
- (16) Hirai, M.; Hirai, R. K.; Iwase, H.; Arai, S.; Mitsuya, S.; Takeda, T.; Seto, H.; Nagao, M. *J. Phys. Chem. Solids* **1999**, *60*, 1359.
- (17) Komura, S.; Takeda, T.; Kawabata, Y.; Ghosh, S. K.; Seto, H.; Nagao, M. *Phys. Rev. E* **2001**, *6304*.
- (18) Huang, J. S.; Milner, S. T.; Farago, B.; Richter, D. *Phys. Rev. Lett.* **1987**, *59*, 2600.
- (19) Hellweg, T.; Langevin, D. *Phys. Rev. E* **1998**, *57*, 6825.
- (20) Gradzielski, M.; Langevin, D. *J. Mol. Struct.* **1996**, *383*, 145.
- (21) Gradzielski, M.; Langevin, D.; Farago, B. *Phys. Rev. E* **1996**, *53*, 3900.
- (22) Helfrich, W. Z. *Naturforsch., A: J. Phys. Sci.* **1978**, *33*, 305.
- (23) Kellay, H.; Binks, B. P.; Hendriks, Y.; Lee, L. T.; Meunier, J. *Adv. Colloid Interface Sci.* **1994**, *49*, 85.
- (24) Hiemenz, P. C.; Rajagopalan, R. *Principles of colloid and surface chemistry*, 3rd revision and expanded ed.; Marcel Dekker: New York, 1997.
- (25) Coldren, B. A.; Warriner, H.; vanZanten, R.; Zasadzinski, J. A.; Sirota, E. B. *Langmuir* **2006**, *22*, 2465.
- (26) Wurger, A. *Phys. Rev. Lett.* **2000**, *85*, 337.
- (27) Paunov, V. N.; Sandler, S. I.; Kaler, E. W. *Langmuir* **2000**, *16*, 8917.
- (28) Kawabata, Y.; Seto, H.; Nagao, M.; Takeda, T. *J. Neutron Res.* **2002**, *10*, 131.
- (29) Kitchens, C. L.; McLeod, M. C.; Roberts, C. B. *J. Phys. Chem. B* **2003**, *107*, 11331.
- (30) Bagwe, R. P.; Khilar, K. C. *Langmuir* **1997**, *13*, 6432.
- (31) Bagwe, R. P.; Khilar, K. C. *Langmuir* **2000**, *16*, 905.
- (32) Eastoe, J.; Fragneto, G.; Robinson, B. H.; Towey, T. F.; Heenan, R. K.; Leng, F. *J. Chem. Soc., Faraday Trans.* **1992**, *88*, 461.
- (33) Atik, S. S.; Thomas, J. K. *J. Am. Chem. Soc.* **1981**, *103*, 3543.
- (34) Towey, T. F.; Khanlodhi, A.; Robinson, B. H. *J. Chem. Soc., Faraday Trans.* **1990**, *86*, 3757.
- (35) Sato, H.; Hirai, T.; Komasa, I. *Ind. Eng. Chem. Res.* **1995**, *34*, 2493.
- (36) Hirai, T.; Sato, H.; Komasa, I. *Ind. Eng. Chem. Res.* **1994**, *33*, 3262.
- (37) Hirai, T.; Tsubaki, Y.; Sato, H.; Komasa, I. *J. Chem. Eng. Jpn.* **1995**, *28*, 468.
- (38) Cason, J. P.; Miller, M. E.; Thompson, J. B.; Roberts, C. B. *J. Phys. Chem. B* **2001**, *105*, 2297.
- (39) Kitchens, C. L.; Roberts, C. B. *Ind. Eng. Chem. Res.* **2004**, *43*, 6070.
- (40) Binks, B. P.; Kellay, H.; Meunier, J. *Europhys. Lett.* **1991**, *16*, 53.

- (41) Chu, B. *Laser light scattering: basic principles and practice*, 2nd ed.; Academic Press: Boston, MA, 1991.
- (42) Farago, B.; Richter, D.; Huang, J. S.; Safran, S. A.; Milner, S. T. *Phys. Rev. Lett.* **1990**, *65*, 3348.
- (43) Huang, J. S.; Safran, S. A.; Kim, M. W.; Grest, G. S.; Kotlarchyk, M.; Quirke, N. *Phys. Rev. Lett.* **1984**, *53*, 592.
- (44) Kotlarchyk, M.; Chen, S. H.; Huang, J. S.; Kim, M. W. *Phys. Rev. Lett.* **1984**, *53*, 941.
- (45) Kotlarchyk, M.; Chen, S. H.; Huang, J. S. *Phys. Rev. A* **1983**, *28*, 508.
- (46) Safran, S. A.; Turkevich, L. A. *Phys. Rev. Lett.* **1983**, *50*, 1930.
- (47) Huang, J. S.; Kim, M. W. *Phys. Rev. Lett.* **1981**, *47*, 1462.
- (48) Kaler, E. W.; Billman, J. F.; Fulton, J. L.; Smith, R. D. *J. Phys. Chem.* **1991**, *95*, 458.
- (49) Peck, D. G.; Johnston, K. P. *J. Phys. Chem.* **1991**, *95*, 9549.
- (50) Kawabata, Y.; Nagao, M.; Seto, H.; Komura, S.; Takeda, T.; Schwahn, D.; Yamada, N. L.; Nobutou, H. *Phys. Rev. Lett.* **2004**, *92*, 056103/1.
- (51) Milner, S. T.; Safran, S. A. *Phys. Rev. A* **1987**, *36*, 4371.
- (52) Eastoe, J.; Sharpe, D. *Langmuir* **1997**, *13*, 3289.
- (53) Arleth, L.; Pedersen, J. S. *Phys. Rev. E* **2001**, *6306*.
- (54) Lisy, V.; Brutovsky, B. *Phys. Rev. E* **2000**, *61*, 4045.
- (55) Lisy, V. *Colloids Surf. A* **2003**, *221*, 255.
- (56) Hellweg, T.; Gradzielski, M.; Farago, B.; Langevin, D. *Colloids Surf. A* **2001**, *183–185*, 159.
- (57) Hellweg, T.; Gradzielski, M.; Farago, B.; Langevin, D.; Safran, S. *Colloids Surf. A* **2003**, *221*, 257.
- (58) Kellay, H.; Meunier, J. *J. Phys.: Condens. Matter* **1996**, *8*, A49.
- (59) Lisy, V.; Brutovsky, B.; Zatovsky, A. V.; Zvelindovsky, A. V. *J. Mol. Liq.* **2001**, *93*, 113.
- (60) Farago, B.; Monkenbusch, M.; Goecking, K. D.; Richter, D.; Huang, J. S. *Phys. B (Amsterdam, Neth.)* **1995**, *213*, 712.
- (61) Farago, B.; Richter, D.; Huang, J. S. *Phys. B (Amsterdam, Neth.)* **1989**, *156*, 452.
- (62) Seki, K.; Komura, S. *Phys. A (Amsterdam, Neth.)* **1995**, *219*, 253.
- (63) Farago, B.; Huang, J. S.; Richter, D.; Safran, S. A.; Milner, S. T. *Prog. Colloid Polym. Sci.* **1990**, *81*, 60.
- (64) Nagao, M.; Seto, H.; Takeda, T.; Kawabata, Y. *J. Chem. Phys.* **2001**, *115*, 10036.
- (65) Nagao, M.; Seto, H.; Kawabata, Y.; Takeda, T. *J. Appl. Crystallogr.* **2000**, *33*, 653.
- (66) Lee, C. T.; Psathas, P. A.; Ziegler, K. J.; Johnston, K. P.; Dai, H. J.; Cochran, H. D.; Melnichenko, Y. B.; Wignall, G. D. *J. Phys. Chem. B* **2000**, *104*, 11094.
- (67) http://www.ncnr.nist.gov/programs/sans/data/red_anal.html. NIST Center for Neutron Research: SANS Data Reduction and Analysis Software, 2006; Vol. 2006.
- (68) Nagao, M.; Seto, H.; Shibayama, M.; Yamada, N. L. *J. Appl. Crystallogr.* **2003**, *36*, 602.
- (69) www.ncnr.nist.gov/resources/sldcalc.html.
- (70) Fried, J. R. *Polymer Science and Technology*; Prentice Hall: Englewood Cliff, NJ, 1995.
- (71) Hellweg, T.; Langevin, D. *Phys. A (Amsterdam, Neth.)* **1999**, *264*, 370.
- (72) Howe, A. M.; McDonald, J. A.; Robinson, B. H. *J. Chem. Soc., Faraday Trans. I* **1987**, *83*, 1007.